*Combust. Sci. and Tech.*, 1993, Vol. 93, pp. 223-243
Photocopying permitted by license only



# Mathematical Simulation of a Circulating Fluidised Bed Combustor

P. C. SARAIVA, J. L. T. AZEVEDO and M. G. CARVALHO *Instituto Superior Técnico, Mechanical Engineering Department, Lisbon, Portugal*

**Abstract**—In this paper a mathematical model to describe a Circulating Atmospheric Fluidised Bed Combustor (CAFBC) is presented. For the fast section of the bed, momentum and energy balance equations are used to predict temperature and velocity profiles for gas and particles. The model performs mass balances for the chemical gas species ($O_2$, $H_2O$, $CO_2$, CO and $SO_2$) with consideration on the last being given for retention by limestone particles. A bubbling bed model is considered to simulate the bottom of the CAFBC. The model is applied to typical conditions of a boiler and the results show the expected trends.

## NOMENCLATURE

| | |
|---|---|
| A | —Area ($m^2$) |
| C | —Concentration (moles) |
| $C_p$ | —Specific heat Capacity (J/KgK) |
| d | —Particle diameter (m) |
| $D_g$ | —Diffusion coefficient ($m^2/s$) |
| H | —Bottom region height (m); Heating Value (J/Kg) |
| h | —Convection heat transfer ($W/m^2K$) |
| $k_c$, $k_d$ | —Kinetic rate; Diffusion rate ($s^{-1}$) |
| m | —Particle mass (Kg) |
| P | —Pressure (Pa) |
| T | —Temperature (K) |
| u | —Velocity (m/s) |
| $\dot{m}$ | —Rate of combustion ($Kg/m^2s$) |
| W | —Mass flux ($Kg/m^2s$) |

*Greek*

| | |
|---|---|
| $\delta$ | —Density ($Kg/m^3$) |
| $\varepsilon$ | —Voidage; Emissivity |
| $\mu$ | —Viscosity (Kg/ms) |
| $\rho$ | —Bulk density (fuel and limestone) ($Kg/m^3$) |
| $\rho_i$ | —Density of a chemical specie ($Kg_i/m^{3}_{air}$) |
| $\sigma$ | —Stefan Boltzman constant ($W/m^2K^4$) |

*Subscripts*

| | |
|---|---|
| o | —Initial conditions |
| f | —fuel particles |
| g | —gas |
| l | —limestone particles |
| mf | —minimum fluidization |
| p | —Particle |
| rad | —radiation |
| s | —inert particles |
| v | —volatiles |
| w | —wall |

## INTRODUCTION

Circulating fluidised bed boilers have a number of advantages over conventional bubbling fluidised bed boilers and became an important topic of research. The empirical design of boiler furnaces practiced for many years promoted studies to understand the processes occurring in such equipment. Nowadays, due to restrictive pollution regulation as well as the necessity of high performance and the development of powerful computers, research programs were created.

Investigations on high-velocity fluidization have been conducted by many investigators (see e.g., Yerushalmi and Avidam, (1985), Kwauk *et al.,* (1987), Rhodes and Geldart, (1987)). These models allowed the identification of the circulating fluidised bed structure, with a more dense zone at the bottom and a fast bed above, with higher particle concentrations near the wall region. Kunni and Levenspiel (1990), developed a model for the hydrodynamics which considers three different phases, (dilute particles entrained, ascending and descending clusters), with mass transfer between them. The key parameter in their model is the decay constant for the fall off of bulk density of solids with height in the freeboard. Berruti and Kalogerakis (1989), modelled the fast bed hydrodynamics using a core-annulus theory which is applied to small diameter risers ($d < 0.3$ m) used in catalytic processes.

Wei$\beta$ *et al.* (1987) developed a mathematical model which describes coal combustion in a CAFBC, based on mass and energy balances for a compartment and considers eight chemical species. However, no details are given about the solids distribution in the reactor and no special treatment is given to the bottom region. At the bottom of a circulating fluidised bed there is a dense phase which has particle concentrations typical of a bubbling fluidised bed (see e.g. Kwauk *et al.,* (1987), Kunni and Levenspiel, (1990)). A compilation of all relevant work on the modelling of circulating fluidised beds and conventional bubbling beds is presented by Manno and Rietema (1990).

The present paper proposes a model for a Circulating Atmospheric Fluidised Bed which includes hydrodynamics of the fast bed as well as for a bubbling bed. Combustion, heat transfer and $SO_2$ retention are modelled throughout the reactor (for details see Saraiva (1992)). After this introduction the mathematical model for the fast and bubbling bed are described, followed by the model of $SO_2$ retention by the limestone particles. The model is applied to operating conditions of a typical boiler and the results are discussed. In the last section the conclusions of the present work and future work for the model are outlined.

## MATHEMATICAL MODEL

### *Fast Bed*

The model used for the fast bed region of the combustor was adopted from Chung and Carlson (1981) and extended to a two-zone core-annulus model. In the core, particle velocities are obtained by integration of the equations of motion. When only particle drag and gravitational forces are considered the particle momentum equation can be written as:

$$u_p \frac{du_p}{dx} = \frac{1}{\tau_p}(u_g - u_p) - g \tag{1}$$

where $\tau_p$ is the particle's relaxation time expressed as:

$$\tau_p = \frac{24\delta_p dp^2}{18\mu\, C_D\, Re_p} \tag{2}$$

The drag coefficient is calculated using the well known correlation

$$C_D = \frac{24}{Re_p}(1 + 0,15Re_p^{0,687})\,\varepsilon^{-4.67} \qquad 1 < Re_p < 10^3 \tag{3}$$

The gas phase velocity is evaluated by integration of the momentum equation:

$$u_g \frac{du_g}{dx} = \frac{1}{\tau_f}(u_g - u_f)\frac{\rho_f}{\rho_g} + \frac{1}{\tau_s}(u_g - u_s)\frac{\rho_s}{\rho_g} - (u_p - u_g)\,S_{burn} \tag{4}$$

where momentum exchange between the gas and particles phase is considered and including the source of momentum exchange due to coal combustion, $S_{burn}$.

For combustion calculations the energy equations for both phases are used to predict the temperature profiles. The evolution of coal particles is assumed to be in three steps. In the first one, coal particles are dried (in this step temperature is assumed constant and equal to 100° C) and heated until the devolatisation temperature. Then devolatisation starts and this process is kinetically controlled. When devolatisation is complete, char combustion is considered to be controlled by both kinetics and oxygen diffusion to the particle's surface. The energy equation for a particle is based on mass and energy balances and can be written as:

$$Cp_f\, m_f \frac{dT_f}{dt} = A_f\, \dot{m}_{v,c}\,(H_{v,c} - Q_v) + A_f\, h\,(T_g - T_f) + A_f\, \sigma\, \varepsilon_f\,(T_g^4 - T_f^4) + H_{H_2O}\frac{d\dot{m}_{H_2O}}{dt} \tag{5}$$

where $Q_v$ represents the fraction of the particle heat of combustion which is transferred to the particle and $\dot{m}_v$ is the mass flow rate released:

$$\dot{m}_v = \frac{\delta_f}{3}\left[1 - \left(\frac{R_c}{R_f}\right)^3\right] R_f A_v \exp\left(-\frac{E_v}{RT_f}\right) \tag{6}$$

for volatile combustion. For char consumption the mass flow rate by combustion, $\dot{m}_c$, is expressed by:

$$\dot{m}_c = \pi\, k_r\, \delta_f\, d_f^2 P_{O_2} \tag{7}$$

where

$$\frac{1}{k_r} = \frac{1}{k_c} + \frac{1}{k_d} \tag{8}$$

$k_c$ and $k_d$ represent the kinetic and diffusion rates. The main assumptions done are: i) the particles are spherical ii) a one-step reaction for combustion iii) the particle density remains constant iv) particles are sufficiently separated from each other that the single-particle combustion analysis is valid for each and v) the temperature of the particle is uniform.

The energy equation for inert particles is similar to equation (5) but without considering the drying, volatilization and combustion steps ($\dot{m}_{v,c} = 0$).

$$C_{ps}\, m_s \frac{dT_s}{dt} = A_s\, h(T_g - T_s) + A_s\, \sigma\, \varepsilon_s\,(T_g^4 - T_s^4) \tag{9}$$

To predict gas phase temperature, an energy balance is performed on a small compartment of height $\triangle x$, leading to:

$$\frac{d}{dx}(\rho_g U_g Cp_g T_g + \rho_f U_f (Cp_f T_f + H_{v,c} - Q_v) + \rho_s U_s Cp_s T_s) =$$

$$\frac{4h}{D}(T_W - T_g) + S_{rad} + Q_{rad} \tag{10}$$

where D is the combustor diameter. The radiative heat fluxes to the combustor walls as well as radiative sources for the gas phase, are evaluated by the Discrete Transfer Method. The overall emissivity is calculated considering the gas as a mixture of grey gases and particles obeying to the Geometrical Optics Theory. The convection coefficient, h, is predicted according to the model of Mahalingam and Kolar (1991) for circulating fluidised beds.

The mass concentrations of fuel and chemical species are expressed as a function of the mass combustion rate:

$$\frac{d}{dx}(\rho_f u_f) = -\frac{3\dot{m}_{v,c}\rho_f}{\delta_f R_f} - a(\rho_f u_f) \tag{11a}$$

$$\frac{d}{dx}(\rho_s u_s) = -a(\rho_s u_s) \tag{11b}$$

$$\frac{d}{dx}(\rho_{O_2} u_g) = -C_1\dot{m}_{v,c} - \frac{M_{O_2}}{2}\frac{d[CO]}{dt} \tag{11c}$$

$$\frac{d}{dx}(\rho_{CO_2} u_g) = C_2\frac{M_{CO_2}}{M_C}\dot{m}_{v,c} + M_{CO_2}\frac{d[CO]}{dt} \tag{11d}$$

$$\frac{d}{dx}(\rho_{CO} u_g) = C_3\frac{M_{CO}}{M_C}\dot{m}_{v,c} - M_{CO}\frac{d[CO]}{dt} \tag{11e}$$

$$\frac{d}{dx}(\rho_{H_2O} u_g) = N_P\frac{dm_{H_2O}}{dt} + C_4\frac{M_{H_2O}}{2M_H}\dot{m}_v \tag{11f}$$

$$\frac{d}{dx}(\rho_{SO_2} u_g) = C_5\dot{m}_{v,c} - C_6K_r \tag{11g}$$

where the constants $C_1$ to $C_5$ are evaluated from stoichiometry. The last term of equation (11a) and (11b) represents the radial diffusion of particles from the core to the annulus. The value of the constant "a" was taken from Rhodes and Geldart (1987). The CO oxidation rate used in equation (11d) was taken from Howard et al. (1973) correlation and the last term of equation (11g) represents the $SO_2$ retention by limestone.

The gas density is related with temperature to a given pressure by the equation of state:

$$\rho_g = P/R_gT_g \tag{12}$$

*Bubbling Bed*

The model adopted for the bubbling bed is a "Level II" model classified as a "learning model" by Van Swaaij (1985). The gas flow is divided into two phases—emulsion and bubble. Mass transfer between the bubble and particle phases is evaluated by a mass

coefficient $k_{be}$, proposed by Sit and Grace (1981), considering diffusive and throughflow effects:

$$K_{be} = \frac{\left[2U_{mf} + 12\left(\frac{D_g \varepsilon_{mf} U_b}{D_b}\right)^{1/2}\right]}{D_b} \tag{13}$$

where $D_b$ is the bubble diameter predicted by a correlation established by Mori and Wen (1975). For a heterogeneous reaction, with negligible particle concentration in the bubble phase, it is assumed that no reaction occurs in the lean phase. Assuming uniform concentration in the particulate phase $C_p$, the gas concentration in the bubble phase $C_b$ can be expressed along the height as:

$$C_b = C_p + (C_o - C_p) \exp\left(-\frac{K_{be} \varepsilon_b x}{\beta U_g}\right) \tag{14}$$

Considering a heterogenous first order reaction with rate $k_r$ in the particulate phase, an overall balance is:

$$U_g\, C_o = \beta\, U_g\, C_{bH} + (1 - \beta)\, U_g\, C_p + k_R\, (1 - \varepsilon_b)\, C_p H \tag{15}$$

The overall rate of carbon consumption may then be expressed as

$$k_R = \sum_i \pi\, d_{fi}^2\, k_{ri}\, F_i\, C_{char} \tag{16}$$

Carvalho *et al.* (1991) established the reaction rate as:

$$\frac{1}{k_r} = \frac{1}{k_c} + \frac{d_f}{\phi\, Sh'\, D'_m} \tag{17}$$

where $Sh'$ is the Sherwood number:

$$\frac{Sh'}{\varepsilon} = \left[4 + 0.576\left(\frac{U_o\, d_f}{D'_m \varepsilon}\right)^{0.78} + 1.28\left(\frac{U_o\, d_f}{D'_m \varepsilon}\right) + 0.141\left(\frac{d_f}{d_s}\right)\left(\frac{U_o\, d_f}{D'_m \varepsilon}\right)^3\right]^{1/2} \tag{18}$$

and the kinetic rate $k_c$ is given by La Nauze (1985);

$$k_c = 0.513\, T_f \exp\,(-9160/T_f) \tag{19}$$

Equations (14) and (15) are solved together to calculate $C_{bH}$ ($x = H$) and $C_p$. The parameter $\beta$ of equations (14) and (15), as well as bubble fraction, $\varepsilon_b$, must be calculated from bed hydrodynamics. A modified two phase theory is used (e.g. Azevedo (1991)) considering the through flow in bubbles (n=3) and the gas velocity in the emulsion is assumed to be larger than the minimum fluidization velocity by a $K_e$ factor correlated for ($\varepsilon_b < .3$) as:

$$K_e = 1 + .25(U_b \varepsilon_{mf}/U_{mf} + 2)\varepsilon_b \qquad (\varepsilon_b > .04) \tag{20}$$

The particulate phase voidage is assumed to remain equal to the incipient fluidization voidage and the bubble velocity is obtained according to Davidson and Harrison (1963):

$$U_b = U_o - U_{mf} + 0.711\sqrt{g\, D_b} \tag{21}$$

Considering the above mentioned modified two-phase theory the bubble void fraction is given by:

$$\varepsilon_b = \frac{U_o - K_e U_{mf}}{U_b + U_{mf}(n + 1 - K_e)} \tag{22}$$

The fraction of flow within the bubbles, $\beta$, is predicted by:

$$\beta = 1 - \frac{U_{mf}\, K_e}{U_o}(1 - \varepsilon_b) \tag{23}$$

The objective of the dense region model is to predict the char concentration in the bed for each class of particles considered and also the mass flow rate due to splashing. Wen and Chen (1982) correlated the entrainment flux of solids at the bed surface as:

$$E_o = 3 \times 10^{-9} D_b (U_o - U_{mf}) \frac{\pi D^2}{4} \frac{\rho_g^{2.5}\, g^{0.5}}{\mu_g^{2.5}} \tag{24}$$

so the mass flux for each size of particles is a function of carbon concentration and mass fraction of each diameter:

$$E_i = E_o \cdot F_i \cdot C_{char} \tag{25}$$

To predict the mass fraction of each class ($F_i$) a mass balance for each size is performed:

$$\left[\begin{array}{c}\text{Falling flux}\\ \text{from fast bed}\end{array}\right] - \left[\begin{array}{c}\text{Ejecting flux from}\\ \text{bubbling bed}\end{array}\right] + \left[\begin{array}{c}\text{Flux from i + 1 size}\\ \text{by combustion}\end{array}\right] -$$

$$\left[\begin{array}{c}\text{Flux from i - 1 size}\\ \text{by combustion}\end{array}\right] - \left[\begin{array}{c}\text{Fraction of combustion}\\ \text{particles burnt}\end{array}\right] = 0$$

which can be written as:

$$W_{fall_i} - E_i + W_{i+1} - W_i - W_{burn_i} = 0 \tag{26}$$

The first term of the above equation is the particle flux of the falling particles related to equations (1) and (11a). The mass flux due to combustion is directly proportional to the reaction rate (see equations (15) and (16)):

$$W_{burn_i} = \pi\, d_{fi}^2\, C_{char} k_{ri}\, C_p O_2\, F_i\, H\, (1 - \varepsilon_b) \tag{27}$$

It is assumed that, from the initial number N of particles of $i^{th}$ size, $N_{i-1}$ will change to $i\text{-}1^{th}$ size and $N_i$ will remain with its original dimensions. The corresponding mass flux from a given size to the smaller one is:

$$W_{i-1} = \frac{H\, \delta_{bed}\, C_{char}}{t_r} \frac{(d_{fi}^3 - d_f^3)}{(d_{fi}^3 - d_{fi-1}^3)} \left(\frac{d_{fi-1}}{d_{fi}}\right)^3 \cdot F_i \tag{28}$$

For the smallest class $W_i = O$ and for the largest $W_{i+1} = 0$. In equation (28) $d_f$ is the particle diameter after the combustion process during a mean particle residence time ($t_r$):

$$d_f = \left(d_{fi}^3 - \frac{6}{\pi} \frac{k_r t_r}{d_f\, C_{char}}\right)^{1/3} \tag{29}$$

Equation (26) can be re-written in the form:

$$A_i F_i + B_i F_{i+1} = C_i \tag{30}$$

forming a set of algebraic linear-equations. The char concentration ($C_{char}$) is calculated from an overall mass balance of the bubbling bed. The bed height is a result of the mass balances of the limestone particles in all the combustor. Since bulk density in the fast bed is calculated, the total mass of solids in the upper region of the combustor is a result of the integration over the total height. Knowing the total amount of solids in the combustor, the dense region height is then calculated.

*$SO_2$ Retention*

During coal combustion, the sulfur compounds are oxidized and the resultant sulfur dioxide is reduced by calcium oxide particles, (produced by the limestone's calcination), forming calcium sulfate according to the reaction:

$$SO_2 + Ca\ O + \frac{1}{2} O_2 \rightarrow Ca\ SO_4$$

The reaction rate of a limestone particle can be expressed as (Borgwardt, (1970)):

$$k_1 = \frac{\pi}{6} d_s^3 k_{vl} C_{SO_2} \tag{31}$$

In equation (31), $k_{vl}$ represents the overall volumetric reaction rate constant and $C_{SO_2}$ is the $SO_2$ concentration in the combustion gases. The overall volumetric reaction rate is calculated by:

$$k_{vl} = 490\ \exp(-17500/R\ T_l) S_g\ \lambda_l \tag{32}$$

where $S_g$ is the specific surface area correlated with calcination temperature (Borgwardt et al (1971)) given by:

$$S_g = -38.4\ T + 5.6 \times 10^4 \qquad T \geq 1253K \tag{33a}$$

$$S_g = 35.9\ T + -3.67 \times 10^4 \qquad T < 1253K \tag{33b}$$

and $\lambda_l$ is the limestone's reactivity which is a function of the fractional conversion of CaO, temperature and particle size.

## NUMERICAL PROCEDURE

The set of non-linear differential equations governing momentum and energy in the fast bed are solved using the Runge-Kutta method. Equations (11a) to (11g) are manipulated by the introduction of equation (11a) into equations (11c) to (11g). By direct integration, the gaseous species are calculated in each compartment. For $SO_2$ retention, the reaction rate is evaluated at all the compartments and mass balances are performed.

In the bubbling bed, the set of algebraic linear equations written in the form of equation (30) is solved directly assuming the char concentration in the bed. Thus an overall mass balance is performed to predict the new char concentration and an iterative procedure is established.

The initial conditions for the fast bed are taken from the feed conditions and from the solids splashing from the bubbling bed. For the bubbling bed calculation, the flux of

TABLE I
Operating Conditions

| Conditions | Mass Flow |
|---|---|
| Air | $\lambda = 1.2$ |
| Fuel ($Kgh^{-1}$) | 480 |
| Additives ($Kgh^{-1}$) | 15.3 |

TABLE II
Coal Composition

| | Coal |
|---|---|
| Lower Heating Value (MJ/Kg) | 9.85 |
| $H_2O$ (%) (raw) | 53.60 |
| Ash (%) (raw) | 3.2 |
| Volatil Matter (%) | 49.40 |
| C(%) (waf) | 66.30 |
| H(%) (waf) | 4.76 |
| S(%) (waf) | 0.46 |
| N(%) (waf) | 0.97 |
| O(%) (waf) | 27.20 |

incoming particles is the sum of the falling flux of solids and the downflow of particles near the walls of the fast bed.

The coal particles are considered in a discrete number of sizes which are tracked along the fast bed height. Each particle size is partially burned out in each passage in the combustor and its diameter is thus reduced. The recirculated particles are considered in the size classes closer to the diameter at the end of the previous passage. The size classes include diameters down to the size which are completely burned in one passage. The procedure considered allows the consideration of only two kinds of coal particles along the combustor, the ones in the first passage which are still releasing moisture and volatiles and the recirculated ones with char combustion.

## DISCUSSION OF RESULTS

The model described in the previous section was applied to a typical circulating fluidised bed boiler. The overall dimensions are 9,4 m high, and a cross-sectional area varying from 0,16 $m^2$ (at the distributor) to 0,42 $m^2$ (at 3,1 m height and above). The combustion air is supplied through the distributor (primary air) and at the secondary air inlets at 0,7 m, 2,7 m, 5,5 m and 7,1 m.

Most of the energy released by the combustion of air and fuel is radiated to the walls covered by water tubes. It is assumed that the boiler's walls have tubes at uniform temperature. In the present work the bubbling bed temperature was fixed at 1123 K. The operating conditions and coal composition used are shown in tables 1 and 2, respectively. The results of the bubbling bed section are not analysed in detail in the present work. This module was introduced in the calculation procedure to allow for the calculation of the gas and reacting particles' initial conditions for the fast bed.

The outlet gas concentrations from the bed are shown as the initial conditions for the fast bed section after dilution with the secondary air (24.8% of the total). The downflow

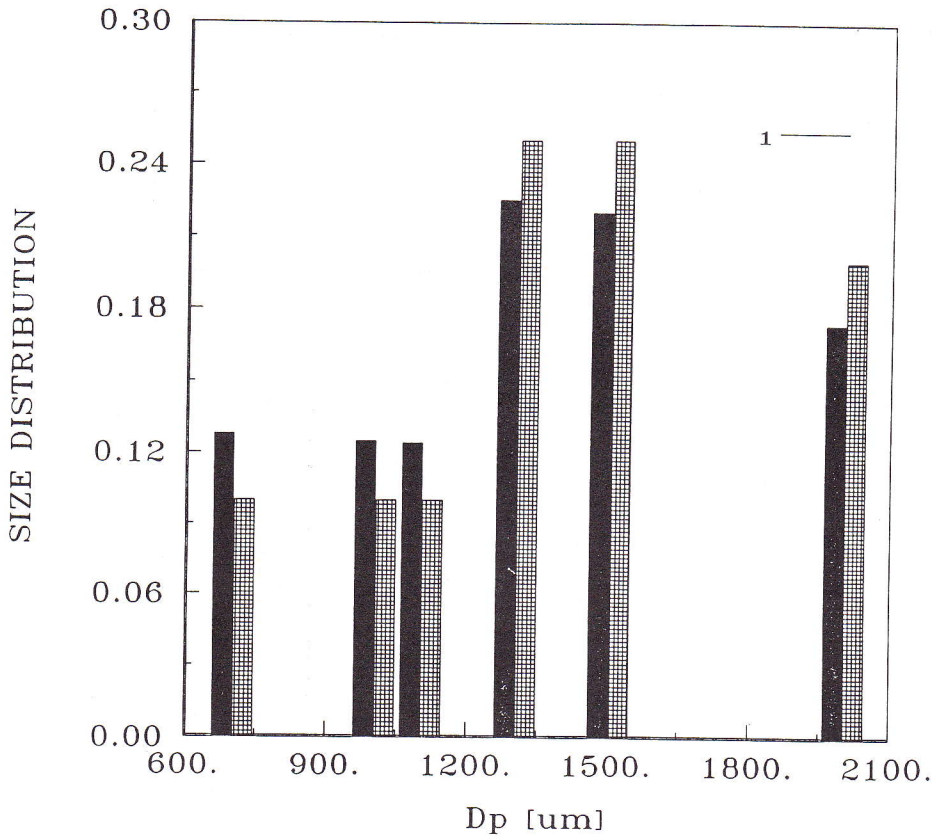


FIGURE 1 ■—Bed; □—Feed

solids near the walls (and calculated from equations (11a) and (11b)), together with the falling particles, is the total feed rate to the bubbling bed.

The char in the bed was found to be about 2.8% of the total weight. The particle size distribution of the feed coal and the resultant in the bed are represented in Figure 1. The projected solids have a particle size distribution similar to the one existing in the bed and the initial particle velocity was taken as twice the bubble velocity.

The predicted temperature profiles along the fast bed of the combustor are presented in Figure 2. The inlet temperature of feed, splashed and recirculated coal particles is about 373 K, 1100 K and 700 K, respectively. The feed coal particles are dried and heated in the initial zone of the fast bed leading to a slight decrease in the gas temperature until coal particles ignite. The volatiles released from the coal particles falling in the bed were assumed to be burned instantaneously at the bed surface. For the splashed and recirculated particles, only char combustion is considered since drying and devolatisation are complete in the first passage in the combustor and during the residence time in the bed. Due to these particles, the gas temperature remains almost constant along the whole combustor, which is typical for CFBC. The figure also shows that the drying time is not negligible and takes about 20-25% of the particle's residence time in the first passage on the combustor.

Figure 3 represents particles' and gas velocities. The gas velocity evolution is a direct consequence of the gas temperature and gas/particle interactions. The drift velocity is

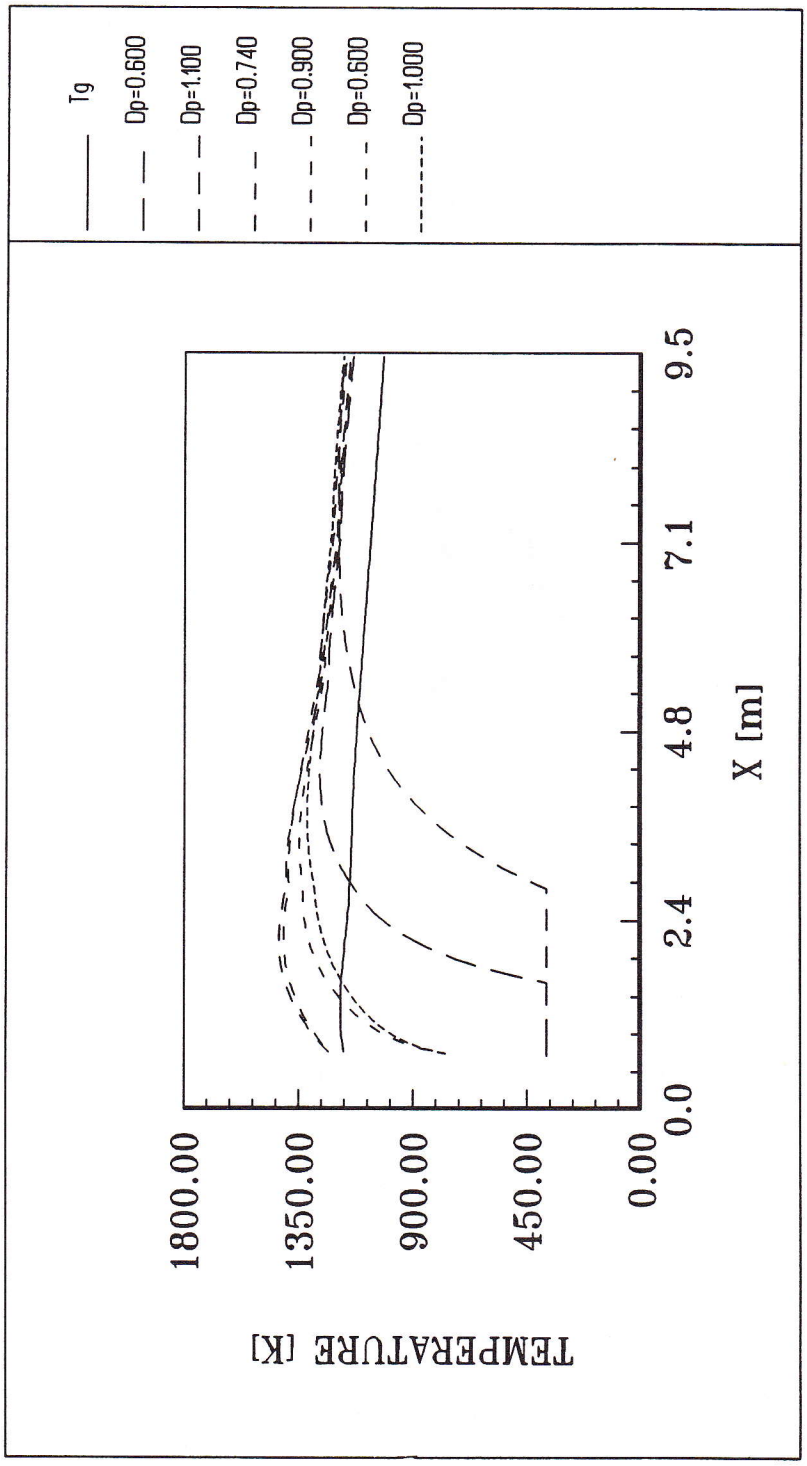


FIGURE 2 Temperature profiles. The dashed lines are representing fresh ($T_{fo}$ = 100 K), recirculated ($T_{fo}$ = 770 K) and projected ($T_{fo}$ = 1123 K) particles for different dimensions.

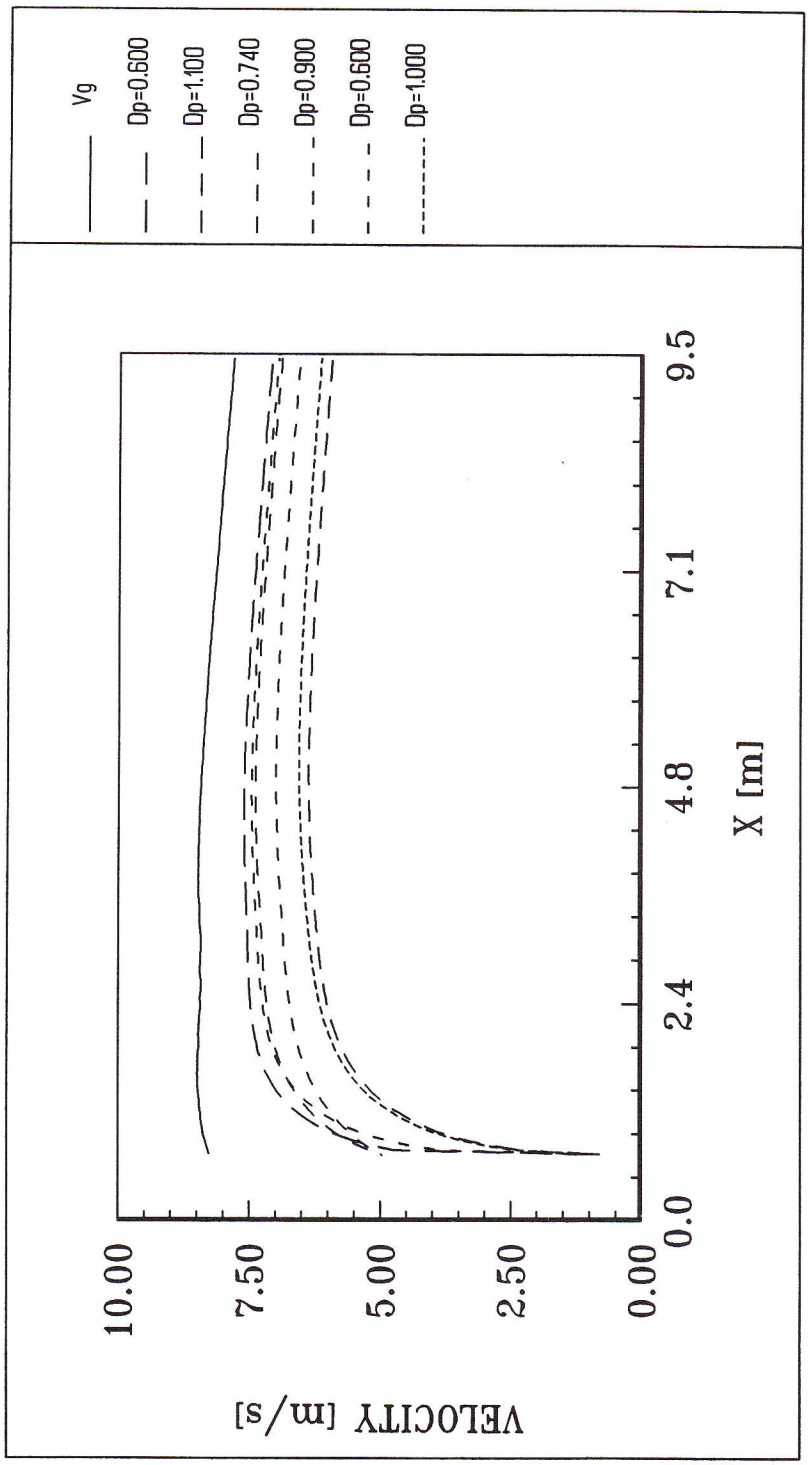


FIGURE 3 Velocity profiles. The dashed lines are representing fresh ($d_f$ = 600 $\mu$m and 1100 $\mu$m and 900 $\mu$m).

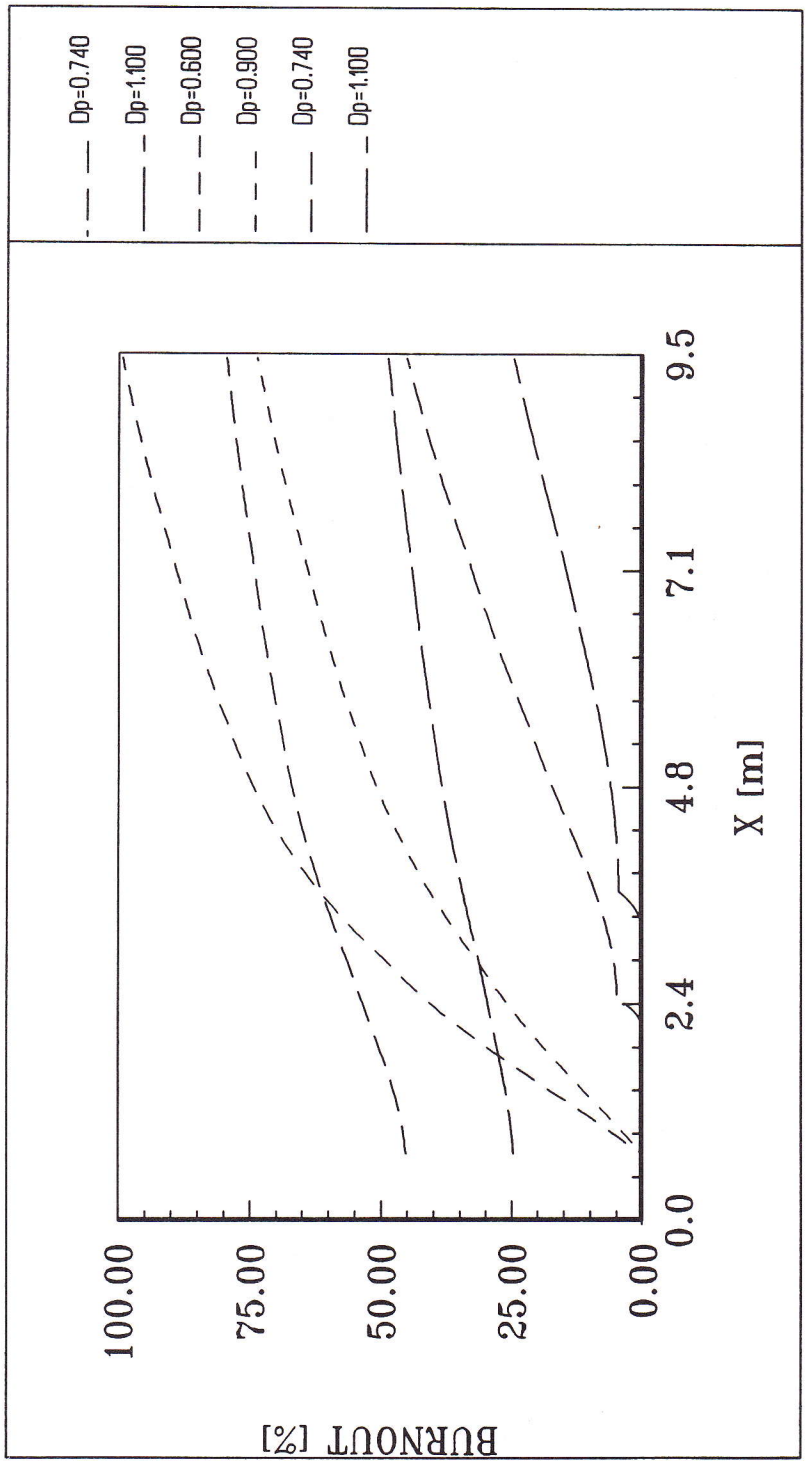


FIGURE 4 Coal Particles Burn-Out: fresh ($d_f$ = 740 $\mu$m and 1100 $\mu$m), projected ($d_f$ = 600 $\mu$m and 900 $\mu$m) and recirculated ($d_f$ = 740 $\mu$m and 1100 $\mu$m)

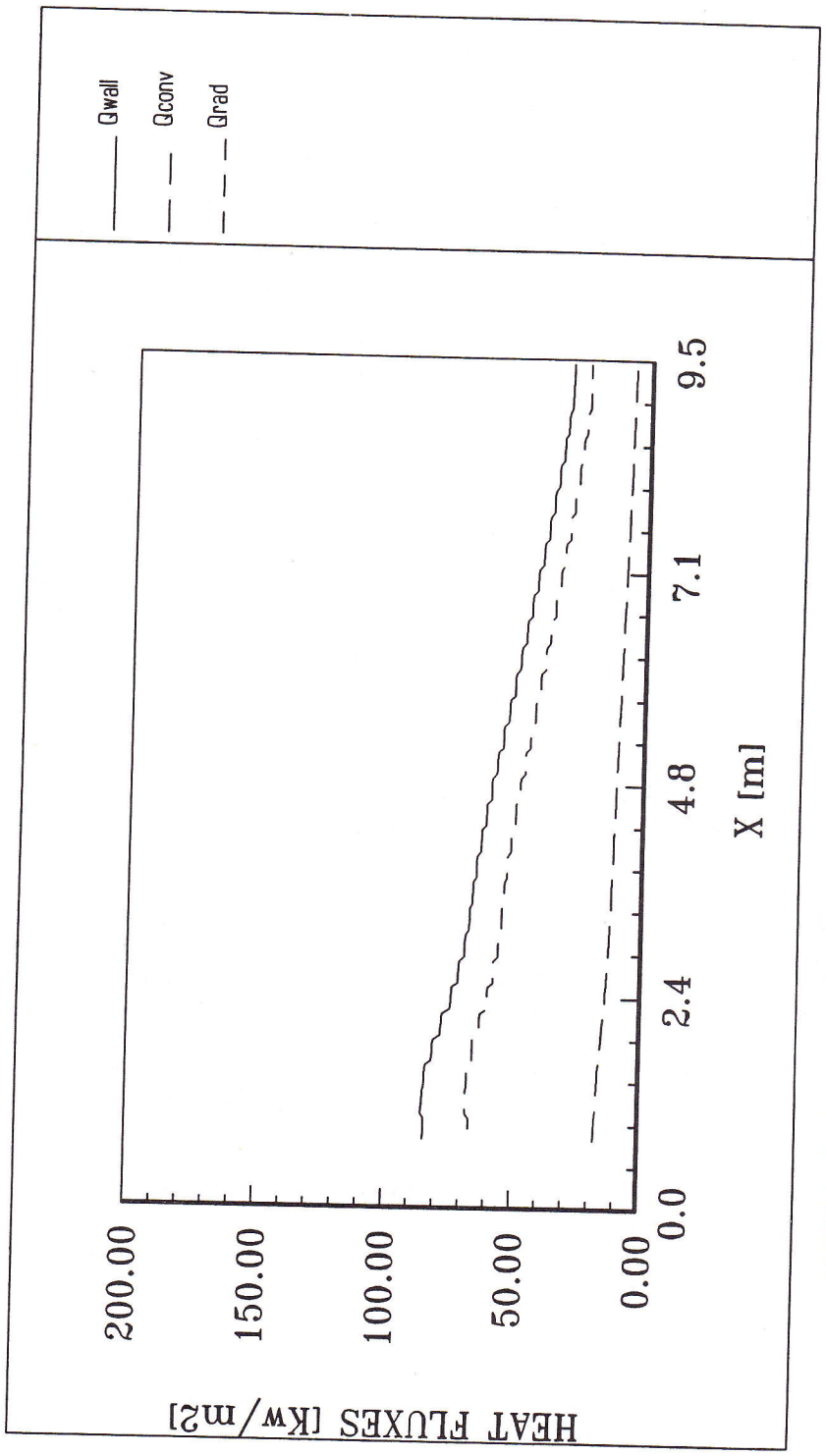


FIGURE 5 Heat Flux to the Walls; Radiative Heat Flux to (about 70% of the total); Convective Heat Flux (about 30% of the total)

higher for the feed particles leading to a high initial acceleration allowing the dynamic equilibrium to be reached in the first two meters of the combustor. For the smallest diameters, higher velocities are reached and the limestone particles have considerably smaller velocities due to their larger density.

Figure 4 represents profiles of predicted burnout, for the coal entrained from the feed, splashed and recirculated, function of particle diameter. It is clear that the fresh particles are not totally consumed, especially the larger ones. The residence time in the fast bed is very small in one passage. However, typical particles in a CAFBC make tens, or even hundreds, of circuits before leaving the system, with each circuit requiring 2 to 20 seconds in the riser (fast bed) and minutes in the return system providing a high residence time. The inclusion of a recirculation model shows that recirculated particles have higher burnout levels depending on their dimensions (50% for 1100 $\mu$m and 85% for 740 $\mu$m). These recirculated particles represent all the passages of coal particles after the initial one. In these passages only the char combustion is considered which allows a common treatment for particles with different residence times. The total degree of burnout is dictated mainly by the cyclone efficiency which is considered in this test with $\eta = 1$. However, the highest burnout levels are reached by the projected particles from the bottom region, since they have dried and released volatiles before.

Heat flux profiles to the walls are shown in Figure 5. It can be seen that 70% of the total heat flux to the walls is by radiation transfer while the other 30% is transferred by convection. Since the operating conditions are typical of low loading, the bulk density is not very high. In this case the gas/particle mixture is not dense, allowing the radiation to play an important role in the heat transfer process.

Figure 6 shows concentration profiles of $CO_2$, CO, $H_2O$ and $O_2$. In the present model it is assumed that the reaction rate is directly proportional to the reaction rate of coal combustion. The high concentrations of $O_2$ (10% for 20% of excess air) and low levels of $CO_2$ emissions show that there is less combustion in the upper part of the combustor than in the lower one. This result is a consequence of the value "a" in equations (11a) and (11b) since it has been evaluated for different operating conditions. The content of water vapour is high in the flue gases due to the high moisture content in the lignite considered.

The influence of limestone particle size and Ca/S molar ratio on the $SO_2$ retention was studied. Figure 7a) shows $SO_2$ concentration profiles with height. The $SO_2$ profile without limestone retention is represented in curve 1 in the combustor (fast bed) for the case of molar ratio Ca/S equal to two and particle sizes of 150 $\mu$m and 500 $\mu$m, respectively. Figure 7a) shows that more $SO_2$ is retained by the larger particles in the first passage. To analyse these results, Figure 7b), is helpful. Figure 7b) represents the limestone's reactivity which is a function of the fraction of CaO not reacted to form $CaSO_4$. The smallest particles have higher reactivities than the largest particles which means a larger capability to absorb $SO_2$ in the combustion gas, but their residence time in the fast bed is lower. However, considering recirculation, the residence time of particles becomes similar for all particle sizes. Thereby, the retention of $SO_2$ is higher for lower limestone diameters due to the higher reactivity for a given conversion fraction.

Figure 8a) shows the $SO_2$ emission profiles for various Ca/S ratios and a fixed particle size ($d_s = 250$ $\mu$m). It is clear that $SO_2$ emissions decrease with increasing Ca/S ratio. Figure 8b) shows that the reactivity of limestone does not remain similar along the combustor (for the three ratios used), showing the importance of mass flow rate in the fast bed. Decreasing the calcium to sulphur ratio, the conversion of CaO to CaSO4 within the particles is increased

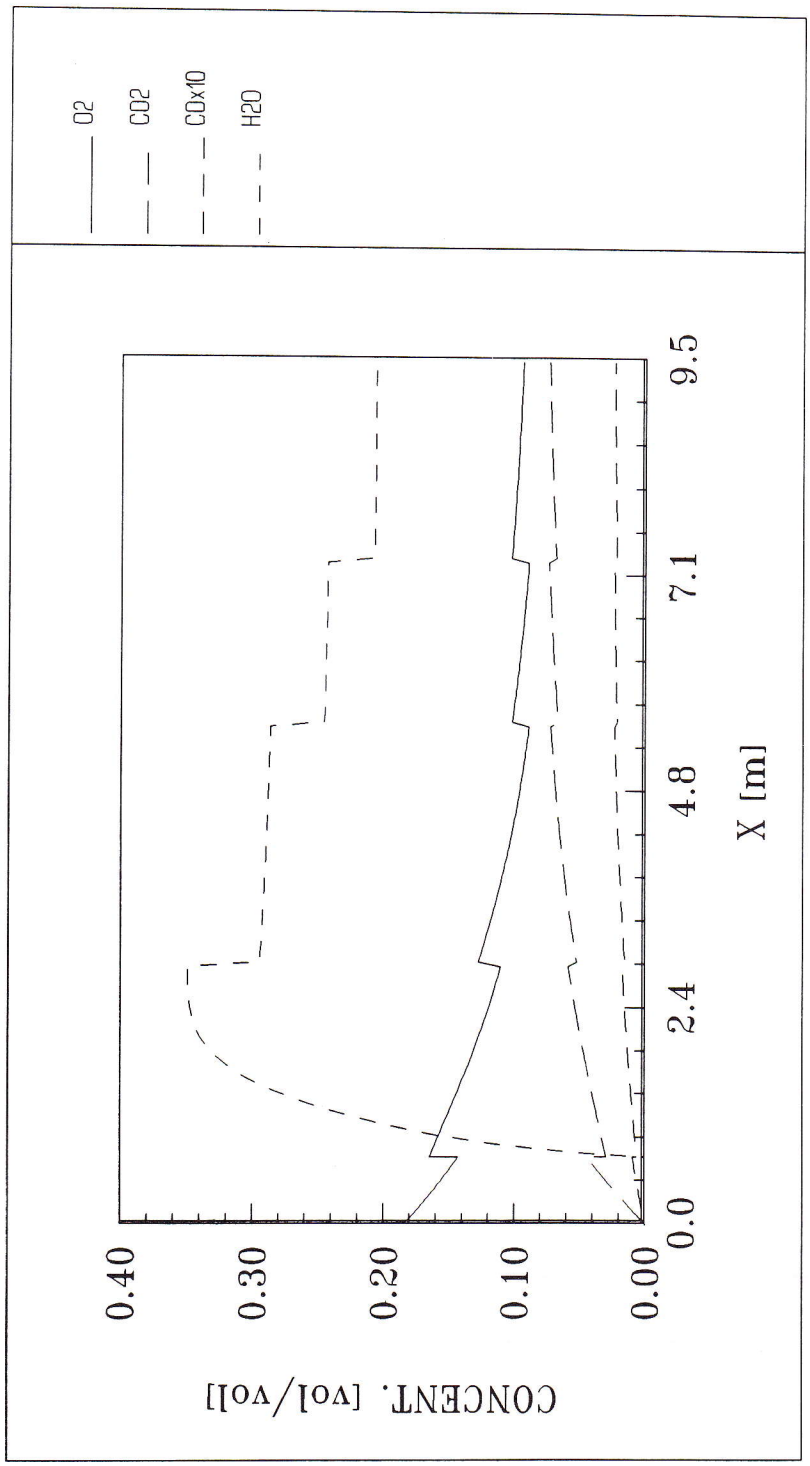


FIGURE 6 $O_2$, $CO_2$, CO and $H_2O$ profiles along the combustor with air staging.

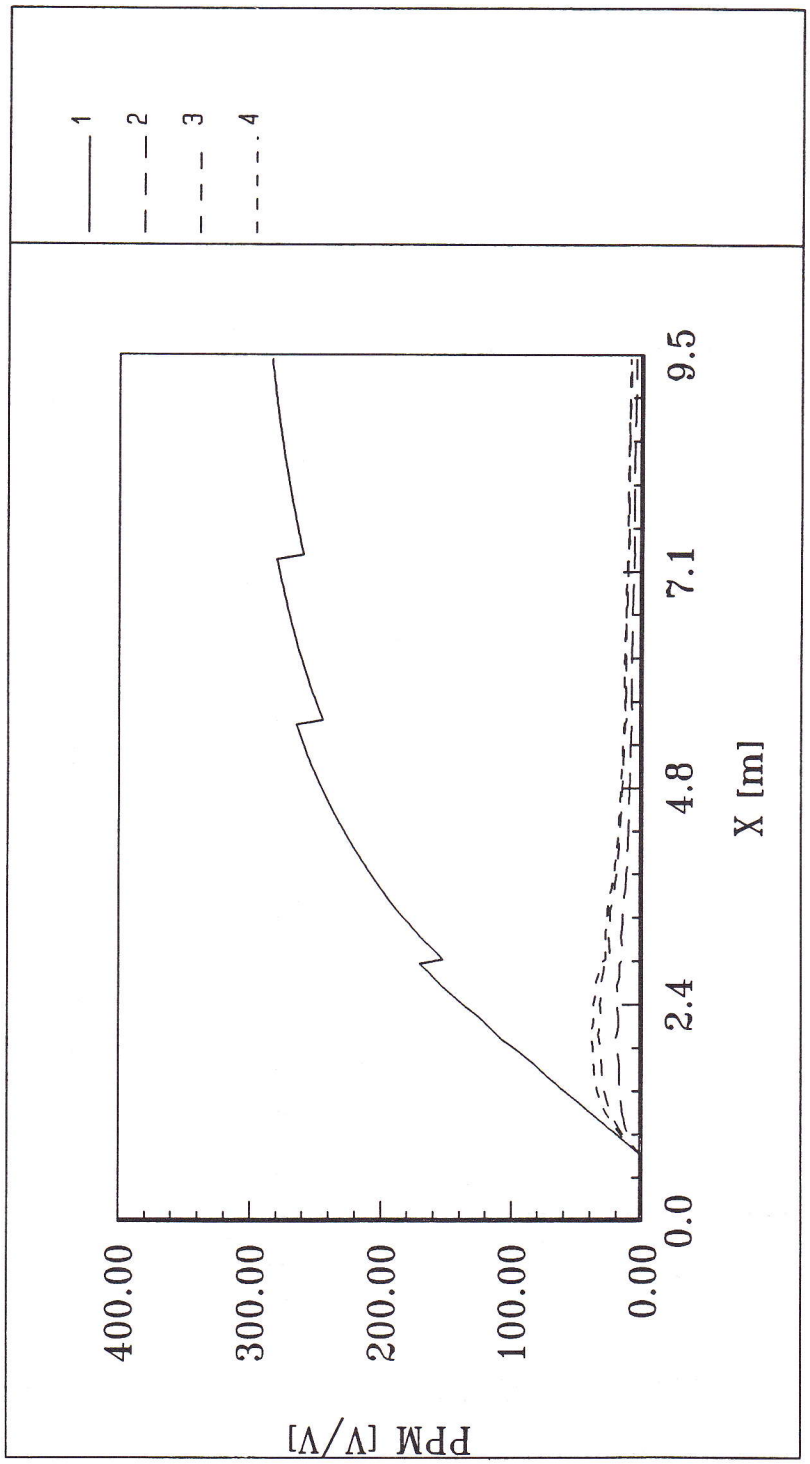


FIGURE 7a) $SO_2$ Emission for the Case of Ca/S = 2:1—Without retention; 2 - $d_1$ = 150 $\mu$m; 3 - $d_1$ = 250 $\mu$m; 4 - $d_1$ = 500 $\mu$m.

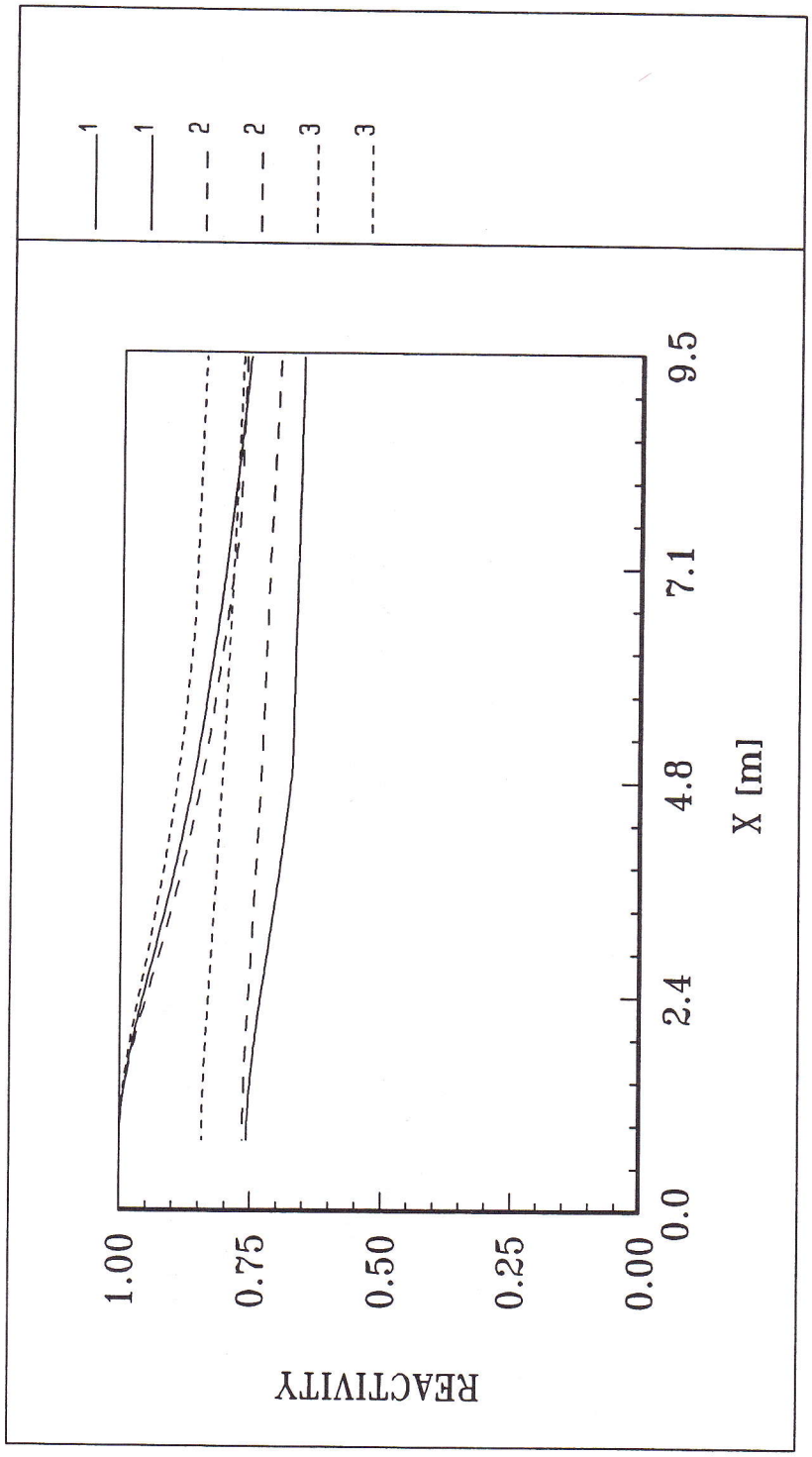


FIGURE 7b) Reactivity of Limestone Particles for the Case of Ca/S = 2; 1 - d1 = 500 $\mu$m; 2 - $d_1$ = 250 $\mu$m; 3 - $d_1$ = 150 $\mu$m.

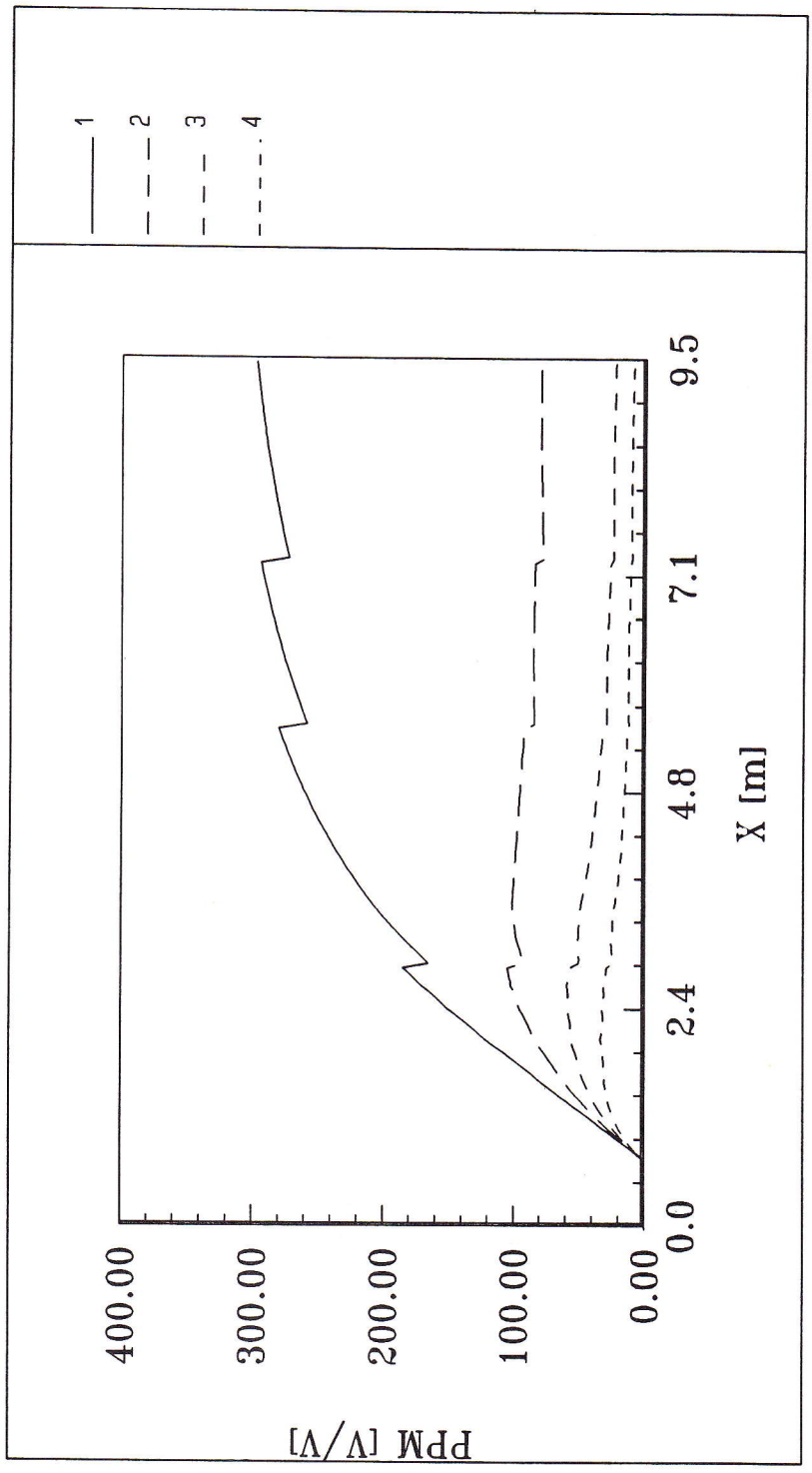


FIGURE 8a) $SO_2$ Emission for the Case of $d_1 = 250\ \mu m$: 1 - Ca/S = 0; 2 = Ca/S = 0.5; 3 - Ca/S = 1; 4 - Ca/S = 2.

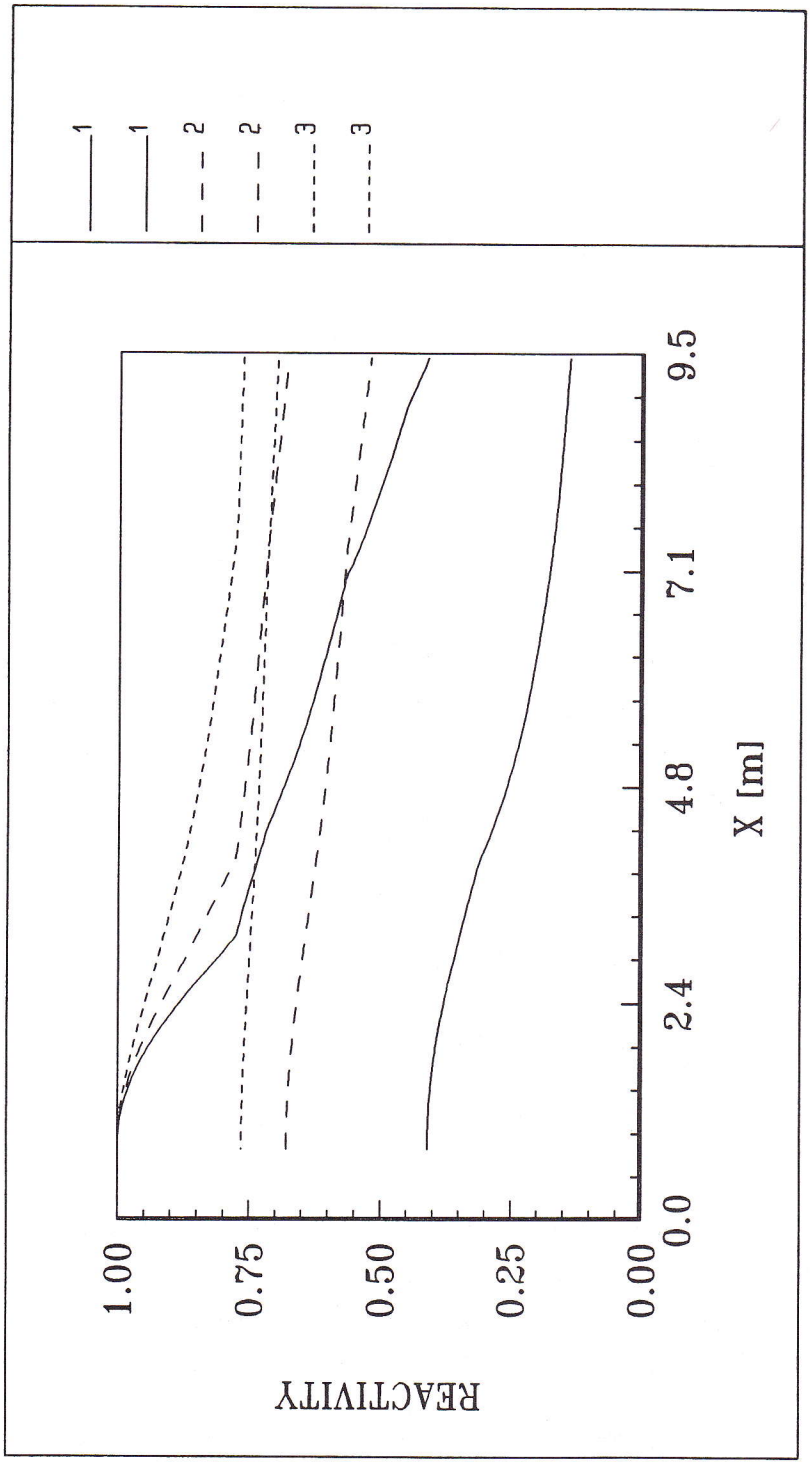


FIGURE 8b) Reactivity of Limestone Particles for the Case of $d_1 = 250$ $\mu$m: 1 - Ca/S = 0.5; 2 - Ca/S = 1; 3 - Ca/S = 2.

## SUMMARY

— A numerical model to simulate a two zone regime with combustion in the fast bed of the CAFBC was implemented. This model was coupled, for the first time, with a model for the bottom region of the combustor derived from bubbling bed theory.
— The model allows for the calculation of gas and particle velocities, gas concentration, temperature and heat fluxes, along the reactor. A model for $SO_2$ retention was also included.
— The model includes some coefficients which are difficult to calculate and therefore empirical values have to be considered. Validation of this model, which is still required, will be performed when experimental results of the furnace considered become available.

ACKNOWLEDGEMENTS

This work is currently supported by the Commission of the European Communities under the contract 0030-C (MB) entitled "Minimization of the Formation of Air Pollutants in the CAFBC by using European Fuels and Additives" of the JOULE subprogram of Solid Fuels. The author P. C. Saraiva wants to express his gratitude to JNICT for the scholarship given for Msc.

REFERENCES

Azevedo, J. L. T., (1991). On the influence of bubble fraction and velocity on bed permeability, IST internal report.

Berruti, F. and Kalogerakis, N., (1989). Modelling the internal flow structure of circulating fluidised bed, *The Can. J. of Chem. Eng.,* **67,** pp. 1010-1014.

Borgwardt, R. H., (1970). Kinetics of the reaction of $SO_2$ with calcined limestone, *Env. Sci. Techn.,* **4,** pp. 49-53.

Borgwardt, R. H., Drehmel, D. C., Kittleman, T. A., Mayfield, O. R. and Owen, J. S., (1971). Selected studies on alkaline additives for sulphur dioxide control, EPA-RTP.

Breault, R. W., Mathur, V. K., (1989). High velocity fluidised bed hidrodynamic modelling, *Ind. Eng. Chem. Res.,* **28,** pp. 684-688.

Carvalho, J. R. F. G., Pinto, M. F. R. and Pinho, C. M. C. T, (1991). Mass transfer around carbon particles burning in fluidised beds, *Trans. IChem. E.,* **69,** pp. 63-70.

Chung, P. M. and Carlson, L., (1981). Vertical combustion for particulate refuse, *Numerical Heat Transfer,* **4,** pp. 101-122.

Davidson, J. F., and Harrison, D., (1963). Fluidised Particles, Cambridge, Cambridge University Press, pp. 21.

Howard, J. B., Williams, G. C. and Fine, D. H., (1973). Kinetics of Carbon Oxidation in Post Flame Gases, *14th Symp. (Int.) on Combustion,* The Combustion Institute, pp. 975-986.

Kunni, D. and Levenspiel, O., (1990). Entrainment of solids from fluidised beds, *Powder Technology,* **61,** pp. 193-206.

Kwauk, M., Ningde, W., Youchu, L., Bingyu, C., and Zhiyuan, S., (1987). Fast fluidization at ICM, Circulating Fluidised Bed Technology, pp. 33-45.

La Nauze, R. D., (1985). Mass transfer considerations in fluidised bed combustion with particular reference to the influence of system pressure, *Chem. Eng. Res. Des.,* **63, pp. 219-229.**

Mahalimgam, M. and Kolar, A. K., (1991). Emulsion Layer Model for Wall Heat Transfer in a Circulating Fluidised Bed, *AIChE J.,* **37,** pp. 1139-1150.

Manno, V. P., Rietema, S. M., (1990). An annotated bibliography of fluidised bed combustion modelling information, *Powder Technology,* pp. 23-34.

Mori, S. and Wen, C. Y., (1975). Estimation of bubble diameter in gaseous fluidised beds, *AIChE J.,* **21,** pp. 109-115.

Rhodes, M. J., Geldart, D., (1987). A model for the circulating fluidised bed, *Powder Technology,* **53,** pp. 155-162.

Saraiva, P. C. (1992). Modelação de Combustão, Transferência de Calor e Emissão de Poluentes em Caldeiras de Leito Fluidizado Circulante, Msc Thesis (in Portuguese).

Sit, S. P. and Grace, J. R., (1981). Effect of bubble interaction on interphase mass transfer in fluidised beds, *Chemical Eng. Science,* **36,** pp. 327-335.

Van Swaaij, J. R., (1985). Chemical Reactors, Fluidization, Academic Press, pp. 595-629.

Wei$\beta$, V., Schöler, J. and Fett, F. N., (1988). Mathematical modelling of coal combustion in a circulating fluidised bed reacting, Circulating Fluidised Bed Technology II, pp. 289-298.

Wen, C. Y. and Chen, L. H., (1982). Fluidised bed freeboard phenomena: Entrainment and elutriation, AIChE J., 28, pp. 117-1287.
Yates, J. G., (1983). Fundamentals of fluidised bed chemical processes, Butterworths.
Yerushalmi, J. and Avidam, A., (1985). High Velocity Fluidization, Fluidization, Academic Press, pp. 225-291.